Integrated Wavelet Packet Modulation and Signal Analysis Using Analytic Wavelet Packets

Michael Bauer, René Anselment, Klaus Dostert
Institute of Industrial Information Technology, Universität Karlsruhe (TH)
Hertzstr. 16
76187 Karlsruhe, Germany

***Abstract*—Transmit signals for low-speed PLC may be seriously obstructed by impulsive noise, resulting in a significant degradation of system performance and reliability. In this paper we provide a possible solution to this problem by using Wavelet Packets for integrated signal modulation and analysis. Moreover we show that Analytic Wavelet Packets which are known for superior signal analysis properties are also suitable for modulation.**

***Keywords*—modulation, power line communication, wavelet packets**

I. Introduction

As is generally known the PLC transmission channel poses a challenging environment for communication. Orthogonal Frequency Division Multiplexing (OFDM) has so far proved to be a good means to counter the problems arising from a PLC channel, especially concerning frequency selective channels [1]. However, OFDM is based on the Fast Fourier Transform (FFT) that delivers information on the spectral properties of a windowed signal, but lacks the ability of resolving its behaviour over time. It is therefore extremely sensitive to the most challenging class of noises on a PLC channel, namely impulsive noise. One alternative modulation scheme that could prove to be promising in this context is the Wavelet Packet Transform, because it provides time resolution in addition to frequency resolution. The approach to exploit time resolution within the Wavelet Packet Transform contrasts the using of Wavelet Packets for Wavelet-OFDM as described in [2].

In this paper, we present the Wavelet Packet Transform and its extension, the Complex Wavelet Packet Transform, for general signal modulation as well as signal analysis at the receiver side. In Section II we provide a short overview of the PLC transmission channel and related simplifying assumptions. Section III summarizes the conventional Wavelet Packet Modulation (WPM) first proposed in [3], which is extended to the Complex Wavelet Packet Modulation (CWPM) in Section IV. Section V compares CWPM to WPM and shows the benefits of using CWPM for integrated signal analysis. Finally, Section VI provides a short summary of the results and the conclusion.

II. PLC Channel Model

A general model for the PLC transmission channel has been proposed for example in [4], see Fig. 1.

The transmit signal $s(t)$ is influenced by the time-variant channel impulse response $h(t,\tau)$, that represents a time-variant, frequency-selective transfer function. In addition, the receive signal $r(t)$ contains up to four different kinds of additive noise, where impulsive noise, either periodic or aperiodic, is to be considered the most challenging class of noises due to its generally wide-band characteristics. For the following sections, we make several simplifying assumptions on the general PLC channel that are valid for the frequency range between 9 kHz and 95 kHz, the CENELEC A band as specified in [5].

We assume that the channel transfer function is ideal, i.e. $h(t,\tau)=\delta(t)$. Moreover, narrowband noise and coloured background noise are assumed to be out of the frequency range that can actually be utilized. We focus our discussion on impulsive noise. Fig. 2 displays one example measurement of aperiodic impulsive noise that has been recorded at the busbar of a transformer station. Although it is difficult to generalize the waveform of impulsive noise, we assume that impulsive noise predominantly exhibits transient behaviour and can best be approximated by

$$n(t) = A_0 \cdot \sin(2\pi f_0 t) \cdot e^{-d \cdot t} \tag{1}$$

Here, A_0 is the initial amplitude of the pulse, f_0 is the frequency of the harmonic oscillation, and d is a parameter specifying the decay of the exponential function.

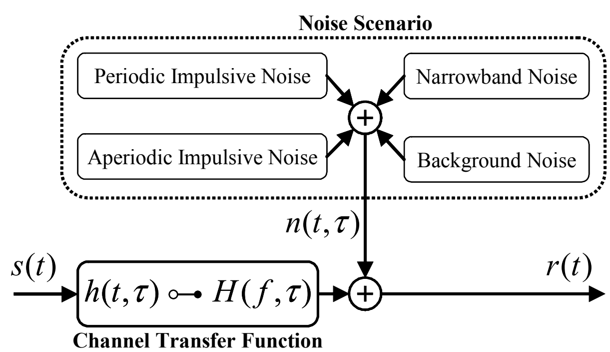

Fig. 1: Model of the PLC transmission channel

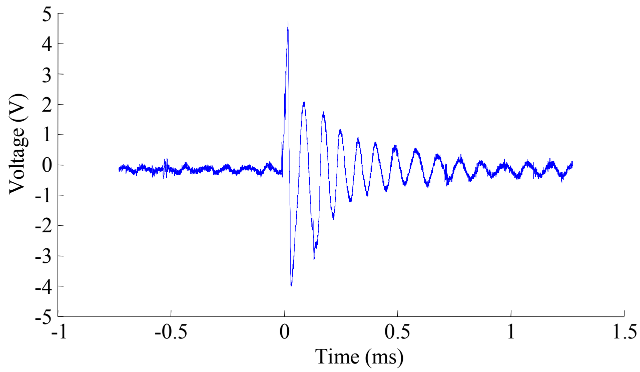

Fig. 2: Waveform of impulsive noise

For the sake of simplicity, we assume d to be large enough so that the waveform decays to values near zero quickly, which guarantees a finite duration of this waveform.

III. CONVENTIONAL WAVELET PACKET MODULATION

The Wavelet Packet Modulation (WPM) has been introduced in [3]. Data symbols consisting of B parallel data sub-streams with individual symbol rates $1/(2^{j_b} T_0)$ with $b = 1,\ldots,B$ are transmitted on B frequency bands using an orthogonal set of wavelet packet functions $p_{j_b,n}^{k_b}(t)$. Here, $1/T_0$ denotes the average symbol rate of all sub-streams.

Each wavelet packet function $p_{j,n}^{k}(t)$ can be derived from an original function $p^k(t)$ through time shifting by an integer multiple n of $2^j T_0$ and through scaling by a factor of 2^{-j}:

$$\begin{aligned} p_{j,n}^{k}(t) &= \sqrt{2^{-j}} \cdot p^k\left(2^{-j}(t - n \cdot 2^j T_0)\right) \\ &= \sqrt{2^{-j}} \cdot p^k(2^{-j} t - n \cdot T_0) \end{aligned} \tag{2}$$

The superscript k consecutively numbers the original unscaled wavelet packet functions in the order of their spectral appearance beginning with $p^0(t) = \phi(t)$ being the only lowpass function called the scaling function.

Although the functions $p_{j,n}^{k}(t)$ significantly overlap in time and frequency, their orthogonality properties ensure reception without intersymbol interference under ideal conditions.

Let the set α contain all combinations (j_b,k_b) which describe the wavelet packet functions supposed to be used for transmission. The transmit signal can then be stated as

$$s_{\mathrm{WPM}}(t) = \sum_{(j_b,k_b)\in\alpha} \sum_{n=-\infty}^{\infty} d_{j_b}^{k_b}(n) \cdot p_{j_b,n}^{k_b}(t), \tag{3}$$

where $d_{j_b}^{k_b}(n)$ is the data symbol transmitted by means of the function $p_{j_b,n}^{k_b}(t)$.

A criterion for α to form a valid wavelet packet basis was given by Coifman, Meyer and Wickerhauser and can be found in [3].

Each function $p_{j_b,n}^{k_b}(t)$ can be expressed in terms of the scaling function $\phi(t)$ filtered by the FIR filter $f_{j_b}^{k_b}(l)$,

$$p_{j_b,n}^{k_b}(t) = \sum_{l=\infty}^{\infty} f_{j_b}^{k_b}(l) \cdot \phi(t - 2^{j_b} n T_0 - l T_0) \tag{4}$$

Equation (3) can be rewritten by using (4) to give an alternative representation of the transmitted signal:

$$\begin{aligned} s_{\mathrm{WPM}}(t) &= \sum_{m=-\infty}^{\infty} \sum_{(j_b,k_b)\in\alpha} \sum_{n=-\infty}^{\infty} d_{j_b}^{k_b}(n) f_{j_b}^{k_b}(m - 2^{j_b} n) \cdot \phi(t - mT_0) \\ &= \sum_{m=-\infty}^{\infty} y(m) \cdot \phi(t - mT_0) \end{aligned} \tag{5}$$

In (5) the sequence $y(m)$ simply is the discrete Inverse Wavelet Packet Transform (IWPT) of the data symbols $d_{j_b}^{k_b}(n)$, which can be efficiently implemented using the well-known filter bank structure introduced by Mallat [6].

This interpretation of (5) leads to a modulation scheme as depicted in Fig. 3. The data symbols are transformed into a time domain signal using a synthesis filter bank with scaling filter $h(n)$ and wavelet filter $g(n)$. The transmitted continuous signal is finally generated by pulse shaping with $\phi(t)$. Mutual relations between $\phi(t)$, $h(n)$, and $g(n)$ can be found in [6].

The FIR filter $f_{j_b}^{k_b}(l)$ merges all filters corresponding to one specific frequency band indexed with b. In this way, together with one upsampling operation by a factor of 2^{j_b}, a compact notation is achieved, as can be seen in (5). Nevertheless, implementation using consecutive stages of upsampling operations by a factor of 2 followed by scaling filter and wavelet filter, respectively, was proved to lead to identical results while being the more efficient way to calculate the time domain signal [6].

Demodulation is depicted in Fig. 4. The received signal is matched filtered by $\phi(-t)$ and sampled with rate $1/T_0$ to get an estimation $\hat{y}(m)$ of the sequence $y(m)$. After that, the Wavelet Packet Transform (WPT), represented by an analysis filter bank structure, recovers the data symbols.

As there are many possible choices for a valid set α, areas in the time-frequency plane can be allocated very flexibly to the data symbols. Fig. 5 displays the resulting structure of the analysis filter bank as well as the corresponding partitioning of the time-frequency plane if the set $\alpha=\{(1,0),(3,4),(3,5),(2,3)\}$ is chosen for modulation and demodulation, respectively.

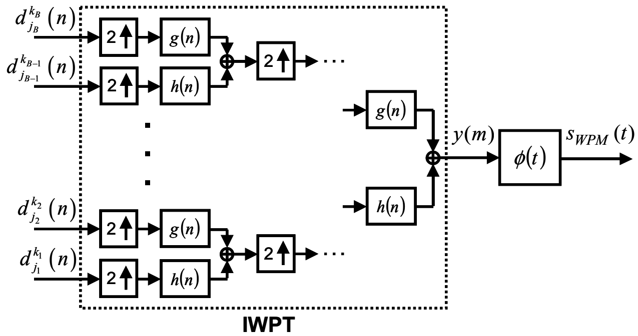

Fig. 3: Block diagram of the WPM modulation tree

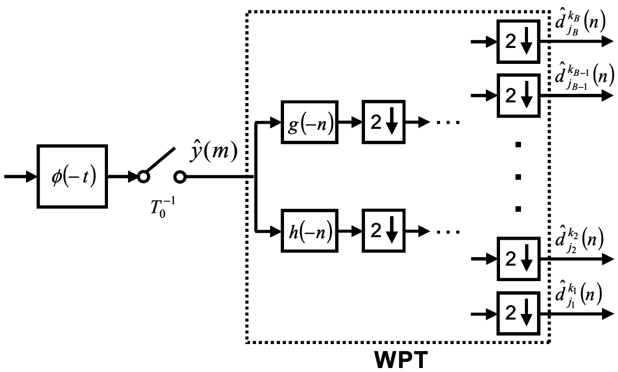

Fig. 4: Block diagram of the WPM demodulation tree

As can be seen from Fig. 5, WPM offers time as well as frequency resolution within one WPM symbol, thereby contrasting conventional multi-carrier modulation schemes like OFDM. Moreover, this time and frequency resolution can be adjusted to current requirements. On the one hand this flexibility proves advantageous for the modulation scheme itself, as the partitioning of the time-frequency plane can be chosen with respect to current characteristics of the channel and the noise scenario [3]. On the other hand, demodulation in a WPM scheme is nothing but time-frequency analysis of the received signal. Useful information about channel and noise scenario can therefore be derived from the wavelet packet coefficients $\hat{d}_j^k(n)$. The potential to adjust resolution in time and frequency gives the WPT an advantage over Fourier based methods also for this application, especially in a scenario with time variant noises such as impulsive noise.

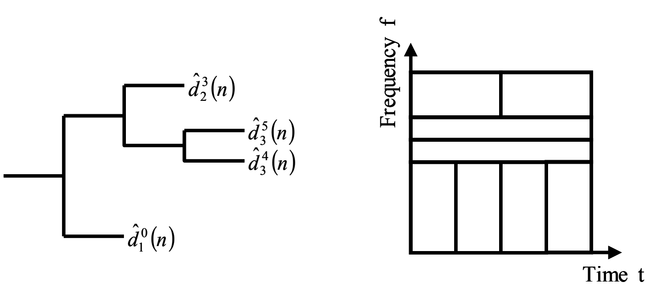

Fig. 5: Possible WPM analysis tree structure and resulting partitioning of the time-frequency plane

IV. COMPLEX WAVELET PACKET MODULATION

Two major problems occur when WPT is used for signal analysis. The transform proves highly shift variant, which is the result of aliasing within a filter bank due to the downsampling operations. Furthermore, the resulting wavelet packet coefficients show oscillations even if a signal with a constant energy distribution is analyzed due to oscillating wavelet packet functions [7].

A possible solution to these problems was proposed in [8]: Instead of real-valued basis functions, approximately analytical and therefore necessarily complex-valued functions are used for calculating the transform. As this cannot be accomplished with one single filter bank, the application of two parallel filter banks for analysis as well as for synthesis is proposed in [8]. One filter bank represents the real part of the transform, the other one represents the imaginary part. Therefore this transform is called "Dual-tree complex wavelet transform". For synthesis the average is calculated to fuse both signals delivered independently by the synthesis filter banks [7]. In order for the basis functions to be analytical, the scaling filters of the two filter banks have to fulfil the so-called half-sample delay (HSD) condition: the imaginary filter bank's scaling filter $h_{(i)}(n)$ has to be identical to the real filter bank's scaling filter $h_{(r)}(n)$, but shifted by half a sample [7]. The scaling filters in the first stage of a filter bank, the so-called "first stage filters", have to be shifted by one sample [7].

As the HSD condition cannot be perfectly fulfilled by FIR filters, the resulting basis functions can only be approximately analytical. Several methods for designing scaling filters which approximately fulfil the HSD condition were proposed e.g. in [9] and [10]. The extension from the approximately analytical Complex Wavelet Transform (CWT) to the approximately analytical Complex Wavelet Packet Transform (CWPT) was carried out in [11]. The well-known tree-like structure of the filter banks remains unchanged but specific filters have to be interchanged between the real and the imaginary filter bank. In [11] a detailed explanation is provided.

When a signal is analysed by means of the CWPT, two sets of coefficients are generated by the dual-tree filter bank. The coefficients at the output of the real filter bank are labelled $d_j^{k(r)}(n)$, the coefficients at the output of the imaginary filter bank are labelled $d_j^{k(i)}(n)$ accordingly. These coefficients result from the analysis of an input signal by means of the real-valued wavelet packet functions $p_{j,n}^{k(r)}(t)$ and $p_{j,n}^{k(i)}(t)$, respectively, which together form an approximate Hilbert pair.

In order to leverage the advantages offered by the CWPT, the complex coefficients need to be calculated. This can be accomplished in two ways:

$$d_j^{k(c+)}(n) = 2^{-1/2}\left(d_j^{k(r)}(n) + j \cdot d_j^{k(i)}(n)\right) \qquad (6)$$

$$d_j^{k(c-)}(n) = 2^{-1/2}\left(d_j^{k(r)}(n) - j \cdot d_j^{k(i)}(n)\right) \qquad (7)$$

These two sets of coefficients correspond to an analysis with the approximately analytical functions

$$p_{j,n}^{k(c+)}(t) = 2^{-1/2}\left(p_{j,n}^{k(r)}(t) + p_{j,n}^{k(i)}(t)\right) \tag{8}$$

$$p_{j,n}^{k(c-)}(t) = 2^{-1/2}\left(p_{j,n}^{k(r)}(t) - p_{j,n}^{k(i)}(t)\right) \tag{9}$$

If the analyzed signal is real-valued, $d_j^{k(c+)}(n)$ is the complex conjugate of $d_j^{k(c-)}(n)$ and therefore does not need to be calculated. Otherwise, the coefficients $d_j^{k(c+)}(n)$ and $d_j^{k(c-)}(n)$ both need to be known in order to uniquely obtain the coefficients $d_j^{k(r)}(n)$ and $d_j^{k(i)}(n)$.

As the CWPT is a linear transform, it can also be written using vector matrix notation [7].

Let the orthogonal matrix $\boldsymbol{F}_{(r)}$ represent the real filter bank and $\boldsymbol{F}_{(i)}$ the imaginary one. Then signal analysis can be described as $\boldsymbol{w}^{(r)}=2^{-1/2}\boldsymbol{F}_{(r)}\cdot\boldsymbol{x}$ and $\boldsymbol{w}^{(i)}=2^{-1/2}\boldsymbol{F}_{(i)}\cdot\boldsymbol{x}$, where the vector $\boldsymbol{x}$ consists of the samples of the time signal which is analysed and the vectors $\boldsymbol{w}^{(r)}$ and $\boldsymbol{w}^{(i)}$ contain the coefficients $d_j^{k(r)}(n)$ and $d_j^{k(i)}(n)$ respectively. Inversely, synthesis can be stated as $\boldsymbol{x} = 2^{-1/2}\cdot\left(\boldsymbol{F}_{(r)}^{-1}\cdot\boldsymbol{w}^{(r)} + \boldsymbol{F}_{(i)}^{-1}\cdot\boldsymbol{w}^{(r)}\right)$.

The coefficients $d_j^{k(c+)}(n)$ and $d_j^{k(c-)}(n)$ are collected in the vectors $\boldsymbol{u}$ and $\boldsymbol{v}$ respectively, where $\boldsymbol{u}=2^{-1/2}(\boldsymbol{w}^{(r)}+j\cdot\boldsymbol{w}^{(i)})$ and $\boldsymbol{v}=2^{-1/2}(\boldsymbol{w}^{(r)}-j\cdot\boldsymbol{w}^{(i)})$.

If CWPT is supposed to be used in a modulation scheme, two approaches seem possible at first glance. On the one hand, data symbols could be interpreted as coefficients $d_j^{k(c+)}(n)$ or $d_j^{k(c-)}(n)$ (approach 1). On the other hand, they could be interpreted as coefficients $d_j^{k(r)}(n)$ or $d_j^{k(i)}(n)$ (approach 2). For both approaches it has to be verified that the dual-tree filter bank in transmultiplexer structure fulfils the perfect reconstruction (PR) condition, i.e. the coefficients can be exactly recovered after a synthesis operation followed by its inverse analysis operation.

Approach 1: Without loss of generality, the data symbols are interpreted as coefficients $d_j^{k(c+)}(n)$, i.e. the vector $\boldsymbol{u}$ contains the data symbols. In order to fulfil the PR condition, the vector $\hat{\boldsymbol{u}}$, resulting from executing dual-tree synthesis of $\boldsymbol{u}$ followed by its dual-tree analysis, must satisfy the condition $\hat{\boldsymbol{u}}=\boldsymbol{u}$. For this condition to be satisfied, both, the real and the imaginary synthesis filter banks must each generate identical outputs so that the averaging operation does not cause any errors. It can be shown that this is satisfied iff

$$\left(\boldsymbol{F}_{(r)}\boldsymbol{F}_{(i)}^{-1} + \boldsymbol{F}_{(i)}\boldsymbol{F}_{(r)}^{-1}\right)\cdot\boldsymbol{v} = \left(\boldsymbol{F}_{(r)}\boldsymbol{F}_{(i)}^{-1} - \boldsymbol{F}_{(i)}\boldsymbol{F}_{(r)}^{-1} - 2j\cdot\boldsymbol{I}\right)\cdot\boldsymbol{u} \tag{10}$$

is fulfilled, where $\boldsymbol{I}$ is the unity matrix.

Numerical tests have shown that it is in general not possible to choose a vector $\boldsymbol{v}$ so that (10) is satisfied, because the matrix $\boldsymbol{M} = \left(\boldsymbol{F}_{(r)}\boldsymbol{F}_{(i)}^{-1} + \boldsymbol{F}_{(i)}\boldsymbol{F}_{(r)}^{-1}\right)$ is very close to being singular for orthogonal scaling filters and wavelet filters that fulfil the HSD condition. This was verified e.g. with so-called q-shift filters from [9] and with filters designed with the common factor method introduced in [10]. All these filters were tested in combination with first stage filters of the Daubechies, the Coiflet, and the Symmlet family. In all cases considered, the determinant of $\boldsymbol{M}$ was shown to be of the order of 10^{-20} and below. Therefore, we postulate that (10) cannot be resolved for arbitrarily chosen data vectors $\boldsymbol{u}$. The data would be required to fulfil certain conditions which renders this modulation scheme generally unfeasible for communications.

Approach 2: Here, the coefficients $d_j^{k(r)}(n)$ or $d_j^{k(i)}(n)$ are supposed to carry the data symbols. Without loss of generality we consider the coefficients $d_j^{k(r)}(n)$ as data symbols in the following. The PR condition for the data vector $\boldsymbol{w}^{(r)}$ is satisfied if $\hat{\boldsymbol{w}}^{(r)}=\boldsymbol{w}^{(r)}$. Again, this is fulfilled if both synthesis filter banks lead to identical output signals, i.e. if $\boldsymbol{F}_{(r)}^{-1}\boldsymbol{w}^{(r)} = \boldsymbol{F}_{(i)}^{-1}\boldsymbol{w}^{(i)}$. Therefore, $\boldsymbol{w}^{(i)}$ has to be chosen according to

$$\boldsymbol{w}^{(i)} = \boldsymbol{F}_{(i)}\boldsymbol{F}_{(r)}^{-1}\boldsymbol{w}^{(r)} \tag{11}$$

As $\boldsymbol{F}_{(r)}$ and $\boldsymbol{F}_{(i)}$ both are orthogonal matrices, their inverses always exist and $\boldsymbol{w}^{(i)}$ can always be chosen to satisfy (11). Moreover, as both filter banks lead to an identical output signal, the result of the imaginary filter bank does not even need to be calculated. As only real-valued wavelet packet functions are actually used for transmission, modulation as well as demodulation can be accomplished using a single synthesis and analysis filter bank respectively. Therefore the proposed modulation scheme is very similar to conventional WPM. Nevertheless, as all requirements for analytical wavelet packet functions, such as the HSD condition, were considered in the filter design process and therefore are met by the filters, a dual-tree filter bank can be optionally used in the receiver for the purpose of signal analysis.

The resulting modulation and demodulation scheme is denoted in Fig. 6. The real and imaginary analysis filter banks are separated by a dashed line.

V. Analysis of Noisy Receive Signals

In order to show the advantages of the proposed CWPM scheme over conventional WPM, we compare the analysis of several receive signals in this section. For this purpose, both systems were simulated in a MATLAB environment.

For the WPM system, Daubechies filters of length 10 were chosen for modulation and signal analysis respectively.

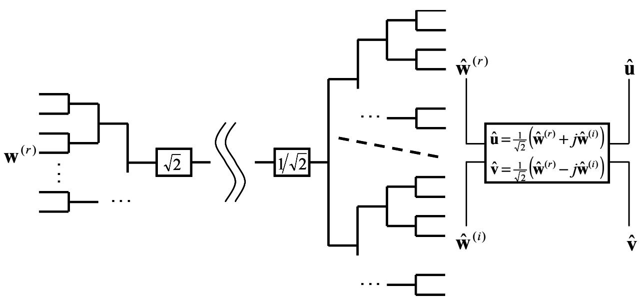

Fig. 6: Diagram of the proposed CWPM scheme. A single-tree synthesis filter bank is used for modulation. A dual-tree analysis filter bank is used for demodulation and signal analysis at the same time

The CWPM system generates the transmitted signal using a single-tree synthesis filter bank structure as depicted in Fig. 6 by means of q-shift filters of length 14 from [9] for modulation as well as for signal analysis. Daubechies filters of length 10 were chosen as first stage filters in order to ensure comparability between both systems.

Whenever a data signal is considered, binary real-valued coding of the data symbols is used, i.e. each symbol is chosen from the set {-1,1}. This corresponds to binary phase shift keying (BPSK) each data symbol.

Both systems use decomposition level 3, i.e. j_b=j=3, for modulating the data symbols. The duration of one WPM or CWPM supersymbol is denoted by T_S, where N data symbols are combined to one supersymbol so that $T_S=N\cdot T_0$.

First, we present an analysis of a pure narrowband noise signal. Narrowband noise is not a typical source of disturbance for the channel under consideration, the results are rather presented for the sake of completeness. In addition, this example shows very clearly the disadvantages regarding signal analysis due to oscillating wavelet coefficients of conventional WPM / WPT.

The noise signal is simulated as a sine-wave of constant power at 25.6 % of the system's Nyquist frequency f_N. Fig. 7 shows the energies $\left|d_j^k(n)\right|^2$ of WPT coefficients on the left and the energies $\left|d_j^{k(c+)}(n)\right|^2$ of CWPT coefficients on the right. Dark areas represent coefficients with high energy, bright areas represent coefficients with low energy. Signal analysis results are shown for decomposition level j=5.

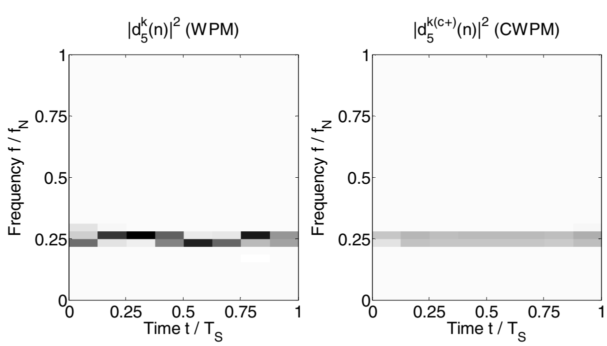

Fig. 7: Signal analysis of narrowband noise

The WPT analysis does not reveal that the power of the noise signal is constant in the relevant time interval, whereas this is clearly visible in the CWPT analysis. This advantage becomes particularly apparent in the analysis of a signal carrying random data and being distorted by the same sine-wave noise signal. Fig. 8 shows the analysis of such a received data signal with a signal-to-noise ratio (SNR) of 2.5 dB.

Here the narrowband noise signal can hardly be detected by WPT analysis due to the underlying data signal. The little number of coefficients with increased energy cannot be allocated to a specific kind of noise. In the CWPT analysis, however, the noise signal can clearly be distinguished from the data signal and can be identified as narrowband noise.

In the following we present the analysis of impulsive noise which is much more typical for PLC transmission channels under consideration. Fig. 9 shows the energies of WPT and CWPT coefficients at decomposition level j=3 when a signal consisting of two noise pulses is analysed. No data signal is considered here, which leads to a more distinct representation of the results. Both pulses are stochastic waveforms of high power during a short period of time. In this case, each pulse has a duration of $0.05\cdot T_S$. The pulses occur at times $0.3\cdot T_S$ and $0.4\cdot T_S$, thereby enclosing a time span of $0.05\cdot T_S$ where noise energy is absent.

Analysis by means of the CWPT clearly shows both pulses and the time span free of noise energy between them. WPT analysis does not allow for distinguishing between the pulses due to oscillations in the coefficients' energies.

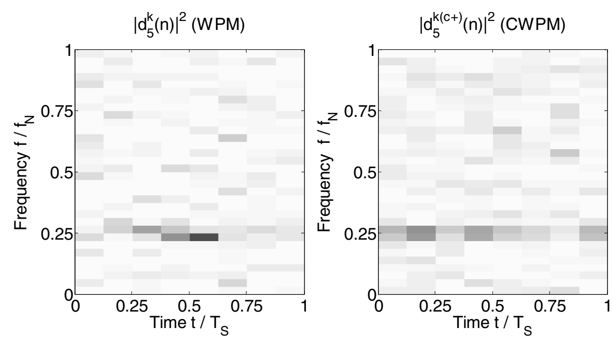

Fig. 8: Analysis of a data signal distorted by narrowband noise

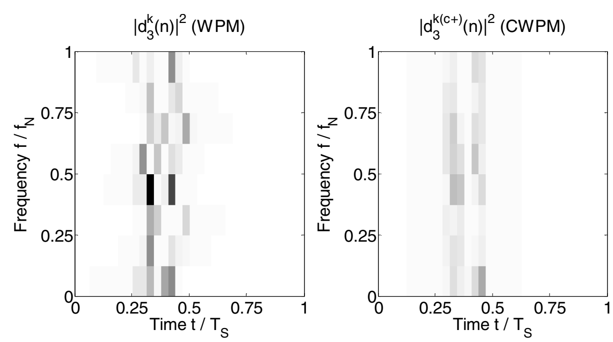

Fig. 9: Analysis of two intermittent noise pulses (stochastic waveforms)

Finally, we present the analysis of noise pulses which are of the type introduced in section II according to (1). A noise signal containing two pulses is superimposed with the data signal. Parameters of the pulses were chosen as follows: The first pulse has initial amplitude of A_0=7, a decay of d=3·10^{-4} and a frequency of f_0=0.64·f_N. It appears after 0.15·T_S. The second pulse which appears after 0.65·T_S has the same parameters, but its initial amplitude is A_0=9. This results in an SNR at the receiver of -5 dB.

The received signal is depicted in Fig. 10. Energies of WPT and CWPT coefficients at decomposition level j=3 are displayed in Fig. 11. The exponential decay of the noise energy can clearly be observed in the CWPT coefficients. The WPT coefficients, however, show oscillations that make the characteristics of the original noise signal hard to estimate.

This can be demonstrated even more explicitly when only the coefficients of the frequency band which contains the major part of the noise energy is regarded. Fig. 12 shows the coefficients' energies of the frequency band with index k=5 at decomposition level j=3. WPT coefficients show sharp notches for indices that correspond to time periods in which the received signal contains large amounts of noise energy.

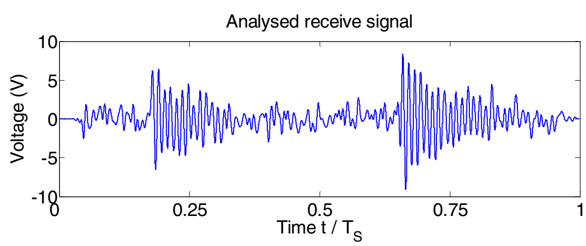

Fig. 10: Data signal distorted by two transient noise pulses

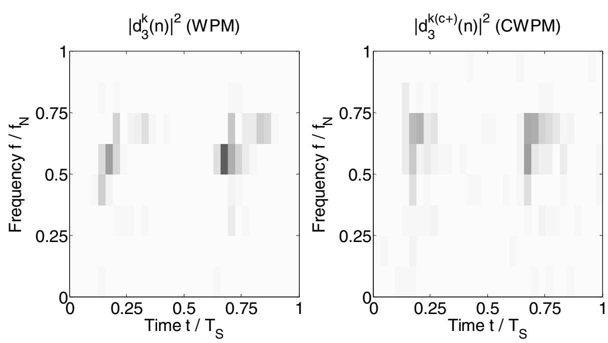

Fig. 11: Analysis of a data signal distorted by transient noise pulses

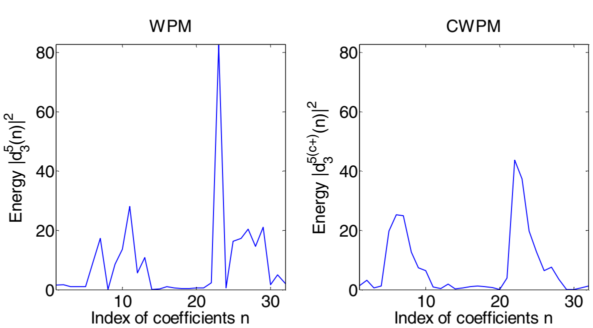

Fig. 12: Coefficients' energy distribution on one specific frequency band

Improved shift invariance properties of CWPT can clearly be seen in Fig. 12 as well. As both noise pulses are similar apart from their different initial amplitudes, the shapes of their respective energy distribution over the CWPT coefficients do not significantly differ. Even the energy ratio of $7^2/9^2 \approx 0.605$ can be estimated very precisely from the CWPT coefficients' energies. This however is not possible regarding energy distribution of WPT coefficients because they show significantly different shapes for the two noise pulses.

VI. Conclusion

In general, it would be desirable to mitigate the influences of channel-related noise on low-speed PLC transmission signals. We proposed an efficient method for integrated data modulation / demodulation and receive signal analysis as a first step towards this goal. The simulation results encourage utilizing Analytic Wavelet Packets for both purposes.

Signal analysis at the receiver side can basically be performed by CWPT in any kind of modulation scheme. However, if CWPM is used for modulation, CWPT analysis can be implemented in an efficient way using the already existing analysis filter bank structure as well as the results provided by the demodulation.

Our proposed modulation scheme therefore allows for leveraging the synergies of the preferable properties of Analytic Wavelet Packets concerning signal analysis along with their applicability for data modulation.

References

[1] K. Dostert, *Power line communications*, Prentice Hall, 2001.
[2] S. Galli, H. Koga, N. Kodama, "Advanced signal processing for PLCs: Wavelet-OFDM," *Proceedings of the 2008 IEEE ISPLC*, pp. 187-192, Jeju City, Korea, April 2008.
[3] A.R. Lindsey, "Orthogonally Multiplexed Communication via Wavelet Packet Bases," Ph.D. Dissertation, Ohio University, Athens, Ohio, June 1995.
[4] M. Goetz, K. Dostert, "A Universal High Speed Powerline Channel Emulator", *International Zurich Seminar on Broadband Communications,* 2002.
[5] CENELEC EN 50065, Signalling on low voltage electrical installations in the frequency range 3 kHz to 148.5 kHz, Brussels, 1991-2002.
[6] S.G. Mallat, *a wavelet tour of signal processing*, 2nd ed., Academic Press, San Diego, California, 1999.
[7] I.W. Selesnick, R.G. Baraniuk and N.G. Kingsbury, "The Dual-Tree Complex Wavelet Transform," *IEEE Signal Processing Magazine*, Vol. 22, Issue 6, pp. 123-151, November 2005.
[8] N.G. Kingsbury, "The Dual-Tree Complex Wavelet Transform: A New Technique for Shift Invariance and Directional Filters," *Proceedings of the 8th IEEE DSP workshop*, paper no. 86, Utah, August 1998.
[9] N.G. Kingsbury, "A Dual-Tree Complex Wavelet Transform With Improved Orthogonality and Symmetry Properties," *Proceedings of the IEEE International Conference on Image Processing*, Vol. 2, pp. 375-378, Vancouver, September 2000.
[10] I.W. Selesnick, "The Design of Approximate Hilbert Transform Pairs of Wavelet Bases," *IEEE Trans. on Signal Processing*, Vol. 50, Issue 5, pp. 1144-1152, May 2002.
[11] T. Weickert, C. Benjaminsen, U. Kiencke, „Analytic Wavelet Packets – Combining the Dual-Tree Approach with Wavelet Packets for Signal Analysis and Filtering," *IEEE Trans. on Signal Processing*, January 2009, in press.